Journal of Power Sources 193 (2009) 315–321

Contents lists available at ScienceDirect

Journal of Power Sources

journal homepage: www.elsevier.com/locate/jpowsour

Optimization strategy for element sizing in hybrid power systems

Alejandro J. del Real*, Alicia Arce, Carlos Bordons

Departamento de Ingeniería de Sistemas y Automática, Universidad de Sevilla, 41092 Sevilla, Spain

ARTICLE INFO

Article history:
Received 20 October 2008
Received in revised form
26 November 2008
Accepted 27 November 2008
Available online 24 December 2008

Keywords:
Hydrogen
Renewable
Hybrid
Power
System
Optimization

ABSTRACT

This paper presents a procedure to evaluate the optimal element sizing of hybrid power systems. In order to generalize the problem, this work exploits the "energy hub" formulation previously presented in the literature, defining an energy hub as an interface among energy producers, consumers and the transportation infrastructure. The resulting optimization minimizes an objective function which is based on costs and efficiencies of the system elements, while taking into account the hub model, energy and power constraints and estimated operational conditions, such as energy prices, input power flow availability and output energy demand. The resulting optimal architecture also constitutes a framework for further real-time control designs.

Moreover, an example of a hybrid storage system is considered. In particular, the architecture of a hybrid plant incorporating a wind generator, batteries and intermediate hydrogen storage is optimized, based on real wind data and averaged residential demands, also taking into account possible estimation errors. The hydrogen system integrates an electrolyzer, a fuel cell stack and hydrogen tanks. The resulting optimal cost of such hybrid power plant is compared with the equivalent hydrogen-only and battery-only systems, showing improvements in investment costs of almost 30% in the worst case.

1. Introduction

The energy infrastructures of today are about to undergo a profound change: fossil fuel prices are raising every year while, at the same time, energy demand increases in every country. Moreover, the aim to reduce greenhouse gas emissions is moving its attention to more environmentally-friendly and sustainable energy sources. With an increased utilization of small distributed energy resources for generation of electricity and heat [1], renewable energy generation will constitute an important part of the overall energy scenario in the coming years.

One of the main problems associated with these kind of systems is the reliability and quality of the power supply. As a matter of fact, since the renewable source is intermittent, unpredictable fluctuations may appear in power output [2]. Also, electrical generation from renewable sources is not subject to demand, which creates imbalance in the system. One way to overcome this problem is by including intermediate storage, such as batteries, water pumping, super-capacitors, compressed air, fly wheels, superconducting magnetic energy storages, etc. [3]. Among the most promising storage technologies are those based on hydrogen production and utilization, which is expected to be used for very different applications [4,5] as they constitute some interesting advantages in terms of cost, autonomy, power range and environmental effects [6].

However, hybrid energy storage systems increase the complexity of the overall power plant, the control design having an important effect on system performance. Thus, there are a number of controllers available in the literature, such as those based on heuristic rules and trial-and-error techniques [7,8]. Fuzzy logic approaches [9,10] are equivalent to those based on heuristic rules in the sense that they rely on system knowledge to obtain the 'best' intuitive power management. Nonetheless, other approaches based on on-line optimization can be found, resulting in a more re-usable and rigorous design process, so that the final algorithm achieves a guaranteed optimum level [11]. Along these lines, an on-line optimization to minimize the hydrogen consumption for residential hybrid power plants was presented in [12,13]. As for renewable sources, the intermittency of the available power also has a great impact on system performance. Although not being suitable for real-time control as the designs cited, there are some control algorithms based on prior knowledge of future conditions (such as wind speed data) which are useful as a basis of comparison for the evaluation of real-time control strategy quality [14].

As well as the control design, it is very important that component sizing be taken into account in order to reduce installation investment costs and to achieve good overall performance, which is the main objective of this work. However, very few papers have addressed this issue. To this end, [15] discusses the best coupling methods for conventional storage batteries with hydrogen energy

* Corresponding author. Tel.: +34 954488161; fax: +34 954487340.
E-mail address: adelreal@cartuja.us.es (A.J. del Real).

0378-7753/$ – see front matter © 2008 Elsevier B.V. All rights reserved.
doi:10.1016/j.jpowsour.2008.11.141

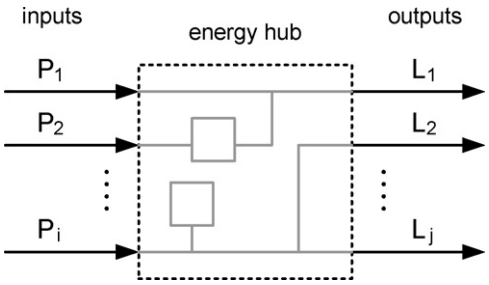

Fig. 1. General energy hub diagram.

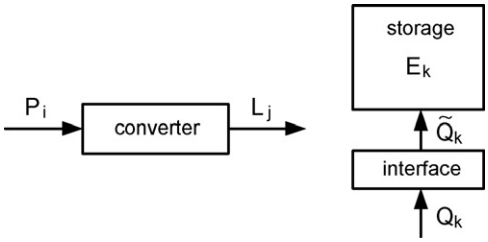

Fig. 2. Energy hub basic elements: converter (left) and storage (right).

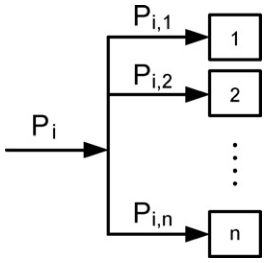

Fig. 3. Input power P_i dispatch.

storage which includes an electrolyzer, hydrogen storage tank, and a fuel cell. The resulting study shows that if multiple energy storage devices with complementary performance characteristics are used together, the resulting hybrid system can dramatically reduce the cost of energy storage over single storage systems. Although [15] is a good study about element sizing, it is only aimed for a certain power system, which makes very difficult to analyze other different system layouts. In contrast, this paper utilizes a very general formulation, which can be used to model and study any possible layout.

In particular, the general sizing problem presented in this paper is a revision of the work presented in [16] and other related papers by the same authors such as [14,17–19], which proposes a general mathematical formulation to model hybrid power plants, introducing the so-called "energy hubs". An energy hub is defined as an interface among energy producers, consumers and the transportation infrastructure. Specifically, [16] finds the optimal hub layout of a power system but does not discuss the sizing problem, while the formulation changes introduced herein are aimed to determine the optimal hub size of a certain layout, thus completing the mentioned previous work. Also, as other of this work contributions, a particular hybrid hydrogen-based power system is optimally sized based on real wind and consumption data. Such system is derived from the general sizing optimization framework proposed.

In the following section, energy hub concept and mathematical formulation are briefly outlined, as there is an extensive literature by the corresponding authors describing them. Section 3 proposes a general cost function to minimize component sizing based on costs and efficiencies. Section 4 applies the general optimization scenario to a wind generator/hydrogen/batteries power plant, also discussing the results obtained. Lastly Section 5 is dedicated to the concluding remarks.

2. Energy hub concept and formulation

As an increased utilization of distributed generation technologies will characterize future energy systems, terms like "multiple energy carrier systems" [20] and "hybrid energy systems" [21] have become the norm when referring to systems including various forms of energy. In this way, as noted in [19], there are a number of approaches to formulate these kind of systems, such as "energy-services supply systems" [22], "basic units" [23], "microgrids" [24] and the so-called "hybrid energy hubs" [25].

The latter formulation is adopted herein, which is extensively described in the PhD thesis [19] and related publications. According to this formulation, energy hubs are defined as interfaces among energy producers, consumers, and the transportation infrastructure (see Fig. 1, where P_i are power inputs and L_j power outputs), and contain three basic elements: direct connections, converters and storage (see Fig. 2, with Q_k being the power exchange, $\tilde{Q}_k$ the internal power and E_k the stored energy).

Converters link inputs and outputs through *coupling factors* $c_{i,j}$, which can be considered to be the converter's steady-state energy efficiency, expressed as:

$$L_j = c_{i,j} P_i \tag{1}$$

Considering all the energy hub inputs **P** and outputs **L**, the following *converter coupling matrix* **C** results:

$$\underbrace{\begin{bmatrix} L_1 \\ \vdots \\ L_i \end{bmatrix}}_{\mathbf{L}} = \underbrace{\begin{bmatrix} c_{1,1} & \cdots & c_{i,1} \\ \vdots & \ddots & \vdots \\ c_{1,j} & \cdots & c_{i,j} \end{bmatrix}}_{\mathbf{C}} \underbrace{\begin{bmatrix} P_1 \\ \vdots \\ P_j \end{bmatrix}}_{\mathbf{P}} \tag{2}$$

As the input flow P_i can be distributed among various converter devices (see Fig. 3), *dispatch factors* $v_{i,n}$ specify how much of the input power P_i flows into the converter n:

$$P_{i,n} = v_{i,n} P_i \tag{3}$$

Conservation of power also introduces the constraints

$$0 \le v_{i,n} \le 1 \quad \forall i, \forall n \tag{4a}$$

$$\sum_n v_{i,n} = 1 \quad \forall i \tag{4b}$$

With respect to storage, power exchange Q_k and stored energy E_k are linked through the equation:

$$\tilde{Q}_k = e_k Q_k = \frac{\mathrm{d}E_k}{\mathrm{d}t} \approx \frac{\triangle E_k}{\triangle t} \triangleq \dot{E}_k \tag{5}$$

e_k being the efficiency of the charge/discharge storage interfaces, expressed as

$$e_k = \begin{cases} e_k^+ & \text{if } Q_k \ge 0 \quad \text{(charging/standby)} \\ 1/e_k^- & \text{else} \quad \text{(discharging)} \end{cases} \tag{6}$$

When storage elements exist, power conservation leads to the following, depending on which side of the converter the storage is located (see Fig. 4):

$$\tilde{P}_i = P_i - Q_i \tag{7a}$$

$$\tilde{L}_j = L_j + M_j \tag{7b}$$

Adding the storage to the hub Eq. (2) leads to:

$$[\mathbf{L} + \mathbf{M}] = \mathbf{C}[\mathbf{P} - \mathbf{Q}] \tag{8}$$

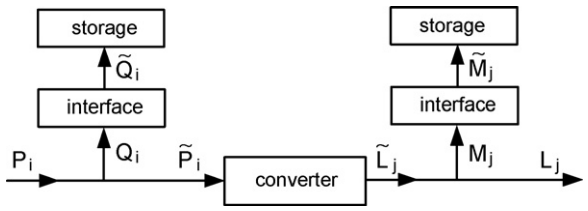

Fig. 4. Converter with storage at the input and the output sides.

Assuming a constant *converter coupling matrix* **C** and applying superposition, the equivalent storage flows are:

$$\mathbf{M^{eq}} = \mathbf{CQ} + \mathbf{M} \tag{9}$$

Rewriting (8) in a more condensed form,

$$\mathbf{L} = \mathbf{CP} - \mathbf{M^{eq}} \tag{10}$$

Defining the *storage coupling matrix* **S** to describe how changes of the storage energy derivatives affect the hub output flows, the equivalent storage power flows $\mathbf{M^{eq}}$ can be stated as

$$\underbrace{\begin{bmatrix} M_1^{eq} \\ \vdots \\ M_k^{eq} \end{bmatrix}}_{\mathbf{M^{eq}}} = \underbrace{\begin{bmatrix} s_{1,1} & \cdots & s_{1,k} \\ \vdots & \ddots & \vdots \\ s_{1,k} & \cdots & s_{k,k} \end{bmatrix}}_{\mathbf{S}} \underbrace{\begin{bmatrix} \dot{E}_1 \\ \vdots \\ \dot{E}_k \end{bmatrix}}_{\dot{\mathbf{E}}} \tag{11}$$

Summarizing all the previous equations, the complete hub energy model would be:

$$\mathbf{L} = \mathbf{CP} - \mathbf{S}\dot{\mathbf{E}} \tag{12}$$

3. Optimal hub size

Optimal hub design can be divided into two different steps: optimal hub sizing and hub control design (see Fig. 5). Most of the papers in the literature, as mentioned in Section 1, are dedicated solely to the controller design, not addressing the sizing problem. The better the controller design, the better the performance of a given system. However, hub sizing and control design are not independent from one another. As a matter of fact, the performance of the overall system not only depends on the quality of the controller but also on the hub characteristics.

Optimal hub sizing for any given hub layout entails optimization of converter and storage element sizes. To that end, cost and efficiencies associated with each component, as well as the estimated working conditions of the hub (such as energy prices, input energy flows availability, output power demand, etc.) have to be taken into account. Such estimated working conditions are usually based on historical data. However, since the optimization is done on estimated power inputs and outputs, estimation errors are likely to occur. Thus, also the sensitivity of the computed optimal size solution to such errors should be taken into account considering a worst-case power availability (input) and consumption (output), which can be done computing the optimization for different estimated conditions data sets and selecting the most conservative hub sizing.

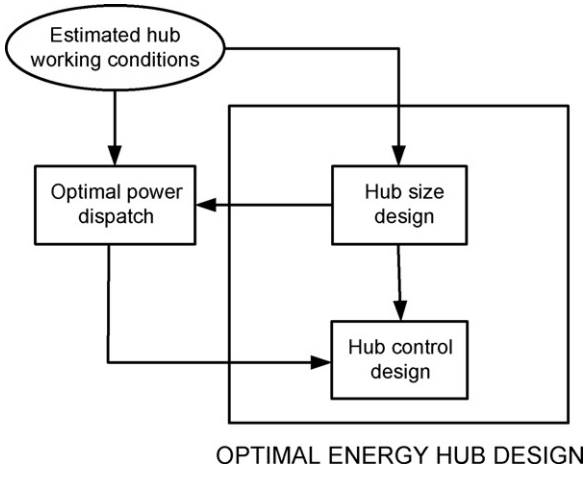

Fig. 5. Optimal energy hub design steps.

Given the optimal hub sizing, a suitable optimization problem minimizing a determined objective function and supposing a set of system operational conditions would then represent the basis of comparison for the evaluation of real-time control strategy quality. This type of optimization problem is referred to as "optimal power dispatch" [14](also shown in Fig. 5).

The problem presented by optimal hub sizing, which is the objective of this work, can be basically expressed with three relations: physical laws representing the hub, its technical limitations, and an objective function which accounts for the minimization of the system investment cost. Then, the optimization is stated as a multi-period nonlinear constrained problem including an objective function, equality and inequality constraints.

The physical laws representing the energy hub are modeled by the equality constraints presented in Section 2. Extending that formulation to consider multiple time periods, the hub model equation would be:

$$\mathbf{L}^{(t)} = \mathbf{C}^{(t)}\mathbf{P}^{(t)} - \mathbf{S}^{(t)}\dot{\mathbf{E}}^{(t)} \quad \forall t \tag{13}$$

Inequality constraints correspond to the technical limitations of the converter and storage elements. Eq. (14a) expresses power conversion limitations of the converters. Eqs. (14b) and (14c) correspond to charging and discharging power limits of the storage interfaces, while (14d) considers the energy capacity limits of the storage devices. The last inequality (14e) is also included so that stored energy at the end of the optimization period N_t is equal to or greater than the initial amount, in order to ensure sustainable storage utilization, where N_t is the last considered period of the optimization.

$$\underline{P}_{i,n} \le \nu_{i,n}^{(t)} P_i^{(t)} \le \bar{P}_{i,n} \quad \forall t, \forall i, \forall n \tag{14a}$$

$$\underline{Q}_i \le Q_i^{(t)} \le \bar{Q}_i \quad \forall t, \forall i \tag{14b}$$

$$\underline{M}_j \le M_j^{(t)} \le \bar{M}_j \quad \forall t, \forall j \tag{14c}$$

$$\underline{E}_k \le E_k^{(t)} \le \bar{E}_k \quad \forall t, \forall k \tag{14d}$$

$$E_k^{(0)} \le E_k^{(N_t)} \quad \forall k \tag{14e}$$

The objective function $\mathcal{F}$ depends on converter and storage element sizes $\bar{P}_{i,n}$, $\bar{E}_k$, $\bar{Q}_i$, $\underline{Q}_i$, $\bar{M}_j$ and $\underline{M}_j$, which are related to the maximum power conversion and storage capacities. Notice that $\underline{Q}_i$ and $\underline{M}_j$ are the maximum discharging rate of the storage interfaces, as $Q_i^{(t)}, M_j^{(t)} < 0$ during discharges and thus $\underline{Q}_i, \underline{M}_j < 0$. Converter and storage elements sizes appear in the cost function multiplied by coefficients $c_{\bar{P}_i}$, $c_{\bar{E}_k}$, $c_{\bar{Q}_i}$, $c_{\underline{Q}_i}$, $c_{\bar{M}_j}$ and $c_{\underline{M}_j}$, which account for the investment cost of hub elements depending on their size. Thus, the solution of the optimization problem provides the optimal sizes of the hub elements, minimizing the total investment cost while taking into account the hub model equations and its technical limitations.

Considering a quadratic function, the objective can be expressed as:

$$\mathcal{F} = \sum_i c_{\bar{P}_i} \bar{P}_i^2 + \sum_k c_{\bar{E}_k} \bar{E}_k^2 + \sum_i (c_{\bar{Q}_i} \bar{Q}_i^2 + c_{\underline{Q}_i} \underline{Q}_i^2) + \sum_j (c_{\bar{M}_j} \bar{M}_j^2 + c_{\underline{M}_j} \underline{M}_j^2) \quad (15)$$

The hub size optimization problem can finally be stated as:

Minimize	objective function
subject to	energy hub model
	energy and power constraints

When the objective function is convex and the constraints are expressed as linear equations, the global optimum can be found utilizing numerical methods, as the solution space is convex.

This approach can be considered as one of the main contributions of this work, as it presents a general optimization framework for element sizing, completing the work initiated in [16] and improving [15] as it only studied a certain system, not a general framework for any system layout as here. Specifically, the formulation changes with respect to [16] are related to the element sizes, which are considered here as optimization variables appearing in the objective function and also in the constraint equation set, as an innovative approach to the sizing problem.

4. Application

Considering the system shown in Fig. 6, the primary energy source is a wind generator, which is connected to a residential load (L_r). The electricity produced via wind (w) can be delivered to the load and/or be diverted to an electrolyzer (E) and batteries (B). The energy consumed by the electrolyzer (Q_E) is used to produce hydrogen, which is stored in the tanks placed in the hydrogen line (E_{H_2}). The fuel cell stack (FC), fed by those tanks, can produce electricity (Q_{FC}). Similarly, the batteries can be charged ($Q_{B,ch}$), storing the energy (E_B), and discharged ($Q_{B,dis}$), thus complementing the total power supplied to the load.

Deriving this specific case from the general problem, and assuming a certain set of operational conditions, the optimal hub sizing for the proposed system is calculated. To that end, the optimization problem is formulated as in the previous Section 3.

4.1. Energy hub model

Model equations are based on the notation presented in Section 2. This way, the specific energy hub is illustrated in Fig. 7. Input, output and storage energy derivative vectors for multiple time periods, can be defined as

$$\mathbf{P}^{(t)} = [P_w^{(t)}] \quad (16)$$

$$\mathbf{L}^{(t)} = [L_r^{(t)}] \quad (17)$$

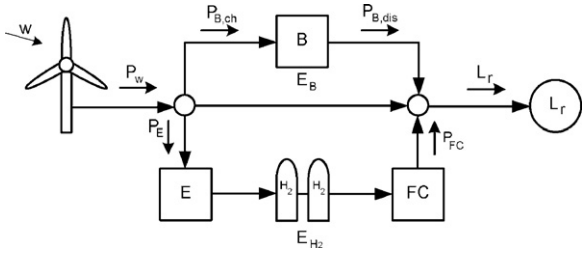

Fig. 6. Hybrid energy storage system.

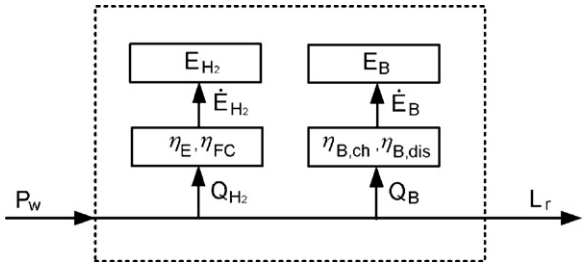

Fig. 7. Corresponding energy hub of a hybrid energy storage system.

Table 1
Hybrid energy storage system efficiencies.

Hub element	Efficiency
Electrolyzer	$\eta_E = 0.74$
Fuel cell	$\eta_{FC} = 0.47$
Battery charging	$\eta_{B,ch} = 0.7$
Battery discharging	$\eta_{B,dis} = 0.9$

$$\dot{\mathbf{E}}^{(t)} = [\, \dot{E}_{H_2}^{(t)} \quad \dot{E}_B^{(t)} \,]^T \quad (18)$$

Also, following the aforementioned notation, *converter coupling matrix* $\mathbf{C}^{(t)}$ and *storage coupling matrix* $\mathbf{S}^{(t)}$ are stated as:

$$\mathbf{C}^{(t)} = [1] \quad (19)$$

$$\mathbf{S}^{(t)} = [\, 1/e_{H_2}^{(t)} \quad 1/e_B^{(t)} \,] \quad (20)$$

where $e_{H_2}^{(t)}$ and $e_B^{(t)}$ are the storage interface efficiencies, the electrolyzer being the 'charging' interface and the fuel cell the 'discharging' interface for the hydrogen line. Also, notice that different battery charging and discharging efficiencies are considered (see Table 1), resulting in the following relations:

$$e_{H_2}^{(t)} = \begin{cases} \eta_E & \text{if } Q_{H_2}^{(t)} \geq 0 \quad \text{(electrolyzer)} \\ 1/\eta_{FC} & \text{else} \quad \text{(fuel cell)} \end{cases} \quad (21a)$$

$$e_B^{(t)} = \begin{cases} \eta_{B,ch} & \text{if } Q_B^{(t)} \geq 0 \quad \text{(battery charging)} \\ 1/\eta_{B,dis} & \text{else} \quad \text{(battery discharging)} \end{cases} \quad (21b)$$

with the power exchanges $Q_{H_2}^{(t)}$, $Q_B^{(t)}$ and storage energy derivatives $\dot{E}_{H_2}^{(t)}$, $\dot{E}_B^{(t)}$ expressed as:

$$\dot{E}_{H_2}^{(t)} = e_{H_2}^{(t)} Q_{H_2}^{(t)} - e_{H_2}^{(t-1)} Q_k^{(t-1)} \quad (22a)$$

$$\dot{E}_B^{(t)} = e_B^{(t)} Q_B^{(t)} - e_B^{(t-1)} Q_B^{(t-1)} \quad (22b)$$

4.2. Energy and power constraints

Technical limitations are modeled as in (14). In this way, input power limits, storage interfaces power exchange capacities and stored energy limitations are evaluated next.

With respect to the input, the constraint vector stated in (23a) incorporates the wind generator model, taking into account that if the wind becomes too strong, the wind generator needs to be switched off and no wind in-feed is apparent to be injected into the system (see Fig. 8). Introducing the function c_w, $W_s^{(t)}$ being the actual wind speed and $P_w^{(t)}$ being the power generated by the wind generator, the input power constraint results:

$$[0] \leq [P_w^{(t)}] \leq [c_w W_s^{(t)}] \quad (23a)$$

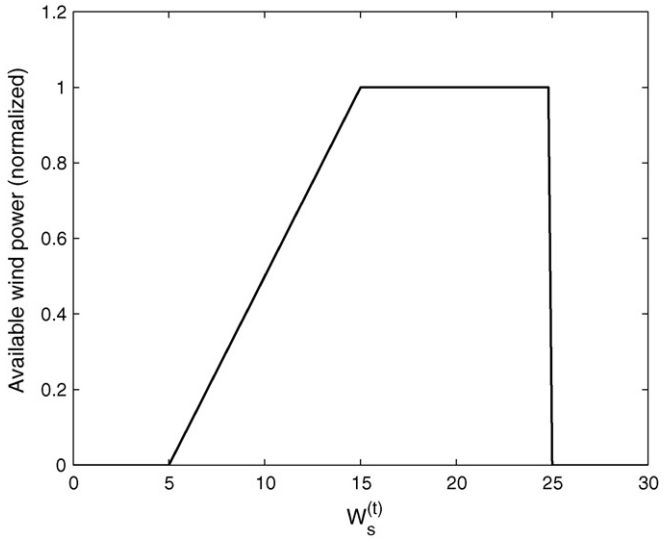

Fig. 8. Normalized wind generator curve.

$$c_w = \begin{cases} 0 & \text{if } W_s^{(t)} < 5 \\ 1/10 - 1/(2W_s^{(t)}) & \text{if } 5 \le W_s^{(t)} < 15 \\ 1/W_s^{(t)} & \text{if } 15 \le W_s^{(t)} < 25 \\ 0 & \text{if } W_s^{(t)} \ge 25 \end{cases} \tag{23b}$$

Power storage exchange is also limited by the maximum power that can be provided by the storage interfaces:

$$\begin{bmatrix} -\bar{Q}_{\text{FC}} \\ -\bar{Q}_{B,\text{dis}} \end{bmatrix} \le \begin{bmatrix} Q_{H_2}^{(t)} \\ Q_B^{(t)} \end{bmatrix} \le \begin{bmatrix} \bar{Q}_E \\ \bar{Q}_{B,\text{ch}} \end{bmatrix} \tag{24}$$

whereas for the hydrogen line, $\bar{Q}_E$ and $\bar{Q}_{\text{FC}}$ represent the maximum capacities of electrolyzer and fuel cell, respectively. Concerning the batteries, $\bar{Q}_{B,\text{ch}}$ and $\bar{Q}_{B,\text{dis}}$ are the limit charging/discharging rates. Notice that these rates are usually a function of total battery size $\bar{E}$, assuming here that $\bar{Q}_{B,\text{ch}} = 0.2\bar{E}$ and $\bar{Q}_{B,\text{dis}} = 2\bar{E}$.

Maximum stored energy depends on the size of the hydrogen tanks $\bar{E}_{H_2}$ and the batteries $\bar{E}_B$. Due to technical constraints, the batteries should never be totally drained nor fully charged; they should always be in a partially charged state. Taking these considerations into account and forcing a safe charge level of $(0.2\bar{E}_B, 0.9\bar{E}_B)$, the constraint can be expressed as:

$$\begin{bmatrix} 0 \\ 0.2\bar{E}_B \end{bmatrix} \le \begin{bmatrix} E_{H_2}^{(t)} \\ E_B^{(t)} \end{bmatrix} \le \begin{bmatrix} \bar{E}_{H_2} \\ 0.9\bar{E}_B \end{bmatrix} \tag{25}$$

Finally, the following constraint to verify sustainable energy storage is also introduced:

$$\begin{bmatrix} E_{H_2}^{(0)} \\ E_B^{(0)} \end{bmatrix} \le \begin{bmatrix} E_{H_2}^{(N_t)} \\ E_B^{(N_t)} \end{bmatrix} \tag{26}$$

4.3. Objective function

Moving from the general (15) to the specific, the objective function would be:

$$\mathcal{F} = c_{\bar{P}_w}\bar{P}_w^2 + c_{\bar{E}_{H_2}}\bar{E}_{H_2}^2 + c_{\bar{E}_B}\bar{E}_B^2 + c_{\bar{Q}_{\text{FC}}}\bar{Q}_{\text{FC}}^2 + c_{\bar{Q}_E}\bar{Q}_E^2 \tag{27}$$

where the cost coefficients are based on the investment costs presented in [15](Table 2).

Table 2
Hybrid energy storage element costs.

Hub element	Investment cost	Cost coefficient
Wind generator	\$2/W	$c_{\bar{P}_w} = 0.2$
Electrolyzer	\$1.9/W	$c_{\bar{Q}_E} = 0.19$
Fuel cell	\$2.5/W	$c_{\bar{Q}_{\text{FC}}} = 0.25$
Hydrogen tank	\$0.03/Wh	$c_{\bar{E}_{H_2}} = 0.003$
Battery	\$0.2/Wh	$c_{\bar{E}_B} = 0.02$

4.4. Operational conditions

As the optimal hub architecture design is based on estimated operational conditions, the more precise the utilized data are, the more accurate are the architectural results. As for the power input, three different wind power normalized data sets were considered (see Fig. 9), which correspond to data recorded during different periods. Concerning the load L_r, the data used is shown in Fig. 10,

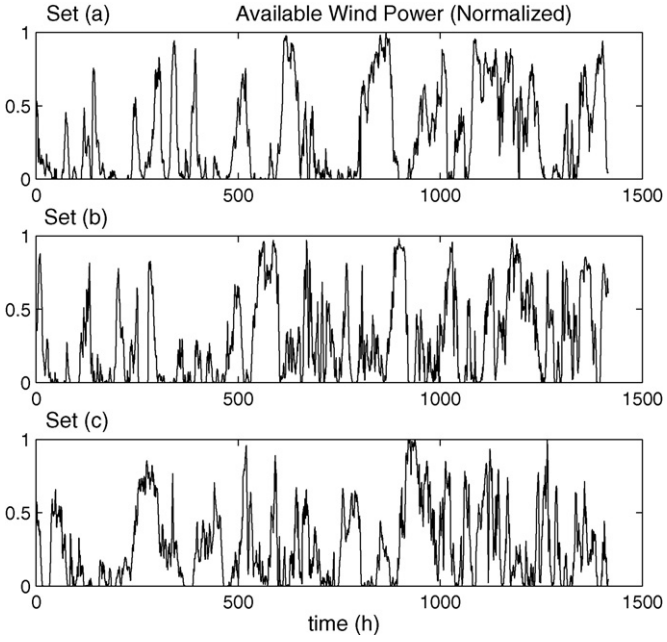

Fig. 9. Normalized wind power data sets.

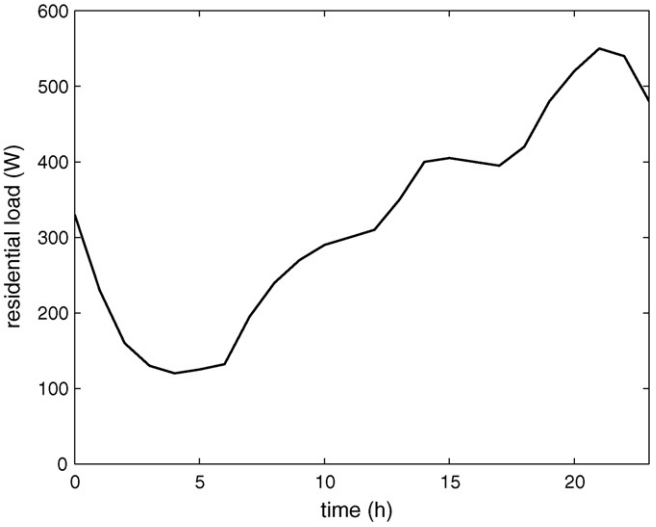

Fig. 10. Residential sector average daily loads.

Table 3
Size optimization results for the hybrid storage system.

	Hybrid system (data set a)	Hybrid system (data set b)	Hybrid system (data set c)
Equipment	Cost (size)	Cost (size)	Cost (size)
Wind generator	$7152 (3576 W)	$7212 (3606 W)	$7600 (3800 W)
Electrolyzer	$617 (325 W)	$623 (327 W)	$656 (345 W)
Fuel cell	$423 (169 W)	$427 (171 W)	$450 (180 W)
H_2 tank	$1545 (51.501 kWh)	$1558 (51.939 kWh)	$1642 (54.730 kWh)
Batteries	$2134 (10.67 kWh)	$2152 (10.67 kWh)	$2268 (11.34 kWh)
Total cost	$11871	$11972	$12616

which represents the average daily load for the residential sector in Spain [26]. The sampling time for all the data sets is 1 h.

4.5. Optimization results

As the objective function is convex and the constraints are expressed as linear equations, the global optimum can be found utilizing numerical methods, as the solution space is convex. Thus, the optimization was implemented in MATLAB using the commercial solver "CPLEX", resulting in a Mixed Integer Quadratic Programming (MIQP). Also, the optimization was performed for the three power input data sets shown in Fig. 9 and the load demand shown in Fig. 10, in order to size the system in the worst possible wind availability scenario.

The results obtained confirm that the third scenario (data set (c) in Fig. 9) is the most disadvantageous, mainly due to the fact that there is less wind power available. Specifically, the investment cost of such scenario is 5.9% higher than the investment cost for the most advantageous conditions, which correspond to data set (a). The optimal size of the hub elements and the investment cost of the installation for the three data sets considered are shown in Table 3.

The hybrid storage system sized for the most disadvantageous wind conditions was simulated for a different wind speed data set,

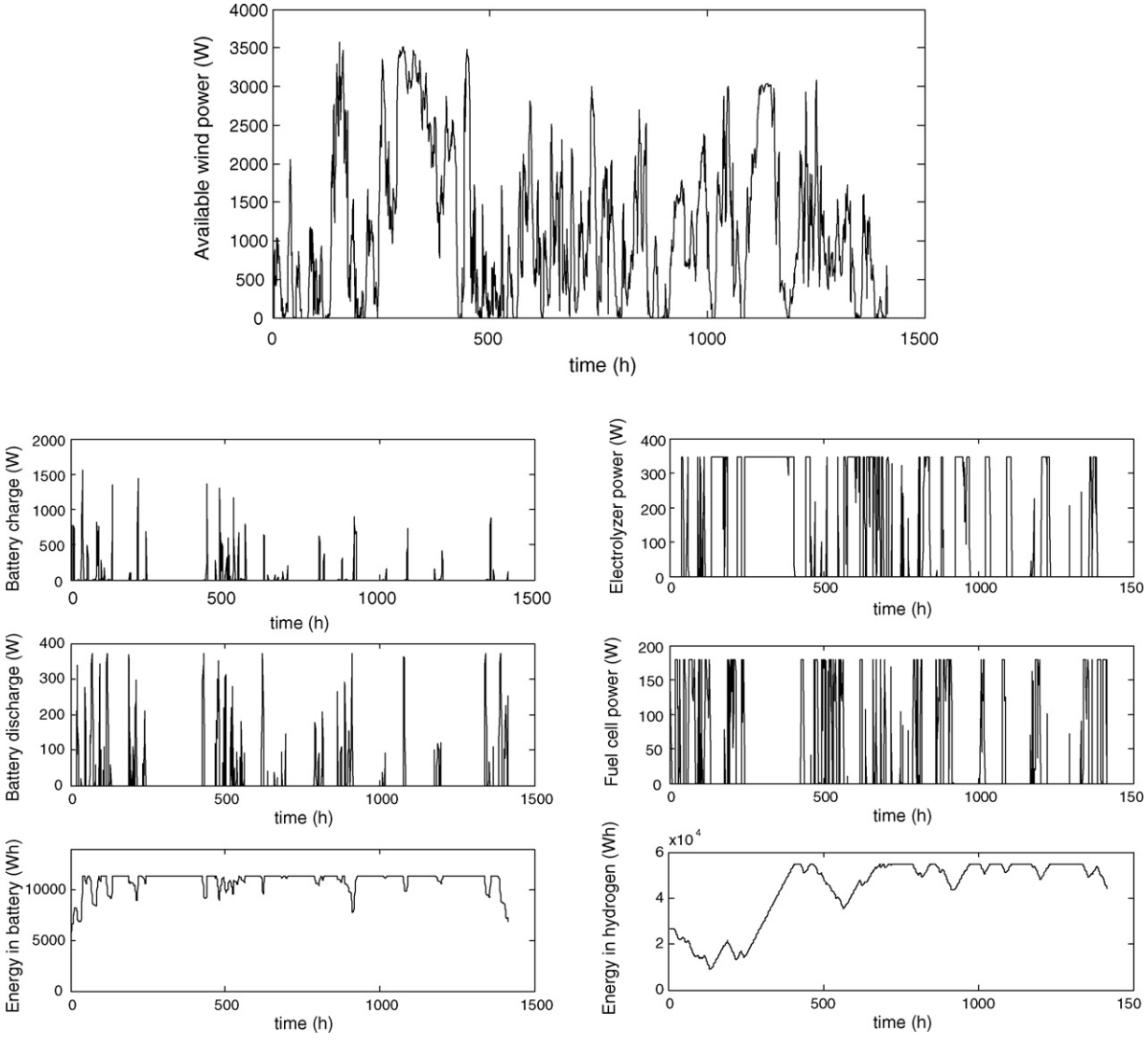

Fig. 11. Optimal power and energy management for a hybrid storage power system.

Table 4
Sensibility analysis.

Estimation error	Oversizing requirement
Peak load demand +1 W	Battery +38.4 Wh
No-wind during +1 h	Electrolyzer +6.47 W
	H_2 tank +382.97 Wh

Table 5
Hybrid system and other layouts comparison.

	Hydrogen-only	Battery-only
Equipment	Cost (size)	Cost (size)
Wind generator	$8600 (4300 W)	$12500 (6250 W)
Electrolyzer	$665 (350 W)	–
Fuel cell	$1375 (550 W)	–
H_2 tank	$3681 (122.695 kWh)	–
Batteries	–	$3651 (18.255 kWh)
Total cost	$14321	$16151
Cost increment	11.91%	28.02%

as can be seen in Fig. 11, which also shows batteries, electrolyzer and fuel cell utilization. In particular, the fuel cell is used as a base power supplier, while batteries are utilized to deliver the power peaks. As expected, the hybrid storage system studied combines the best characteristics of both energy storage devices. It is also remarkable that the system can supply all the power residential demand when simulated with the wind speed data shown in Fig. 11, as such wind speeds resulted to be more advantageous than the wind conditions used to size the system (set data (c) in Fig. 9). The case that the wind conditions were worse than the conditions which the system was designed for is discussed in next Section 4.6.

4.6. Sensibility analysis

Although being done for the worst possible scenario, estimation errors are likely to occur, i.e., if the real conditions are even worse than the conditions considered herein. Thus, a sensibility analysis was performed to take into account these errors and its associated costs. In particular, the analysis was realized considering two error estimations: increments in the load demand during peaks and longer periods without wind available. During such situations, the optimally sized system would not be able to satisfy the power demands. One possibility to overcome these situations is to oversize the system.

Specifically, as the simulations (see Fig. 11) show that batteries are utilized to deliver the power peaks, the battery size should be incremented in order to take into account possible peak load estimation errors. In order to consider wind speed prediction errors, the optimization tests showed that the electrolyzer and the hydrogen tank should be oversized in order to accumulate more hydrogen, which would be available during periods without power from wind. The detailed analysis results are shown in Table 4, taking into account peak load estimation errors of 1 W and no-wind extra periods of 1 h.

4.7. Different layouts comparison

Finally, the optimization was done for two other possible layouts: hydrogen-only and battery-only storage, based on the wind power availability data set (c) shown in Fig. 9 and the load demand presented in Fig. 10. In particular, hydrogen-only storage cost is 11.91% higher than the hybrid plant, the battery-only choice being 28.02% more expensive than such hybrid system (see Table 5 for detailed information). In a hydrogen-only choice, the fuel cell size has to be increased in order to create the power peaks, which results in a cost increase due to the high cost of the equipment. On the other hand, battery-only storage requires a large total energy capacity, which is costly too. Also, as the hybrid system can manage power in a flexible and efficient way, wind generator for such hybrid system can be smaller than the wind generator needed by the two other layouts.

5. Concluding remarks

In this paper, an optimization strategy for sizing hybrid power systems is presented, improving the mathematical formulation based on the "energy hub" concept described in previous literature. The optimization procedure was applied to a hybrid power plant incorporating a wind generator, conventional batteries and a hydrogen storage system comprised of a fuel cell, an electrolyzer and hydrogen tanks. Also, a sensibility analysis was performed to take into account possible estimation errors. Finally, the optimal architecture was compared to other possible layouts, resulting in almost a 30% improvement among the possible system layouts in terms of cost effectiveness, showing the flexibility and usefulness of the improved formulation proposed herein.

References

[1] A.M. Borbely, J.F. Kreider (Eds.), Distributed Generation: The Power Paradigm for the New Millenium, CRC Press, Boca Raton, 2001.
[2] D. Anderson, M. Leach, Energy Policy 32 (2004) 1603–1614.
[3] R. Dell, D. Rand, J. Power Sources 100 (2001) 2–17.
[4] E. Leal, J. Silveira, J. Power Sources 106 (1) (2002) 102–108.
[5] A. Lokurlu, T. Grube, B. Hohlein, D. Stolten, Int. J. Hydrogen Energy 28 (7) (2003) 703–711.
[6] J. Kaldellis, D. Zafirakis, Optimum energy storage techniques for the improvement of renewable energy sources-based electricity generation economic efficiency, Energy, 2007.
[7] J. Vanhanen, P. Kauranen, P. Lund, L. Manninen, Solar Energy 53 (3) (1994) 267–278.
[8] A. Arce, A. del Real, C. Bordons, Power management heuristic control for a hybrid fuel cell vehicle (in Spanish), in: XXVIII Jornadas de Automática, 2007.
[9] K. Jeong, W. Lee, C. Kim, J. Power Sources 145 (2005) 319–326.
[10] A. Bilodeau, K. Agbossou, J. Power Sources 162 (2006) 757–764.
[11] A. Schell, H. Peing, D. Tran, E. Stamos, C. Lin, M. Kim, Annu. Rev. Control 29 (2005) 159–168.
[12] I. Valero, S. Bacha, E. Rulliere, J. Power Sources 156 (2006) 50–56.
[13] A. del Real, A. Arce, C. Bordons, Proceedings of the 2007 Conference on Decision and Control, New Orleans, LA, 2007.
[14] M. Geidl, G. Andersson, Proceedings of the 15th Power Systems Computation Conference, Liege, Belgium, 2005.
[15] S. Vosen, J. Keller, Int. J. Hydrogen Energy 24 (1999) 1139–1156.
[16] M. Geidl, G. Andersson, Proceedings of the IEEE PES PowerTech, Lausanne, Switzerland, 2007.
[17] M. Geidl, G. Koeppel, P. Favre-Perrod, B. Klöckl, G. Andersson, K. Fröhlich, IEEE Power Energy Mag. 5 (1) (2007) 24–30.
[18] M. Geidl, G. Andersson, IEEE Trans. Power Syst. 22 (1) (2007) 145–155.
[19] M. Geidl, Integrated Modeling and Optimization of Multi-Carrier Energy Systems, Ph.D. Thesis, ETH, Zurich, 2007.
[20] B. Bakken, A. Haugstad, K.S. Hornnes, S. Vist, Proceedings of the Scandinavian Conference on Simulation and Modeling, Linköping, Sweden, 1999.
[21] J.F. Manwell, Encyclopedia Energy 3 (2004) 215–229.
[22] H.M. Groscurth, T. Bruckner, R. Kümmel, Energy 20 (9) (1995) 941–958.
[23] I. Bouwmans, K. Hemmes, Proceedings of the 2nd International Symposium on Distributed Generation, Stockholm, Sweden, 2002.
[24] R.H. Lasseter, Proceedings of the IEEE PES Winter Meeting, New York, USA, 2002.
[25] R. Frick, P. Favre-Perrod, Proposal for a multifunctional energy bus and its interlink with generation and consumption, Master's Thesis, ETH, High Voltage Laboratory, Zurich, 2004.
[26] Proyecto INDEL: Atlas de la Demanda Eléctrica Española, Tech. rep., Red Eléctrica de España, 1997.